EDGE ARTICLE

Retro-forward synthesis design and experimental validation of potent structural analogs of known drugs†

Ahmad Makkawi,‡[a] Wiktor Beker,‡[b] Agnieszka Wołos,‡[b] Sabyasachi Manna,[a] Rafał Roszak,[b] Sara Szymkuć,[b] Martyna Moskal,[b] Aleksei Koshevarnikov,[ab] Karol Molga,[b] Anna Żądło-Dobrowolska*[a] and Bartosz A. Grzybowski [ID] *[acd]

Generation of structural analogs to "parent" molecule(s) of interest remains one of the important elements of drug development. Ideally, such analogs should be synthesizable by concise and robust synthetic routes. The current work illustrates how this process can be facilitated by a computational pipeline spanning (i) diversification of the parent *via* substructure replacements aimed at enhancing biological activity, (ii) retrosynthesis of the thus generated "replicas" to identify substrates, (iii) forward syntheses originating from these substrates (and synthetically versatile "auxiliaries") and guided "towards" the parent, and (iv) evaluation of the candidates for target binding and other medicinal–chemical properties. This pipeline proposes syntheses of thousands of readily makeable analogs in a matter of minutes, and is deployed here to validate by experiment seven structural analogs of Ketoprofen and six analogs of Donepezil. The concise, computer-designed syntheses are confirmed in 12 out of 13 cases, offering access to several potent inhibitors. While the synthesis-design component is robust, binding affinities are predicted less accurately although still to the order-of-magnitude, which may be valuable in discerning promising from inadequate binders.

1. Introduction

Recent years have brought revolutionary advances[1–10] in the use of computers to autonomously plan chemical syntheses of arbitrary targets, all the way up to complex natural products.[8–10] One of the prominent areas of application of these algorithms has been in drug discovery where the synthesis design is part of algorithmic pipelines[11–15] intended to predict target and off target binding as well as ADME-Tox properties. While the premium is, without doubt, on discovering potent candidates featuring unprecedented scaffolds[16] and binding modes, many drugs are derivatives of the old ones and "the best way to discover a new drug is to start with an old one".[17] Accordingly, analogs structurally similar to some desired "parent" molecules continue to be sought in drug screening and lead-optimization campaigns[18] and efforts to accelerate this process with the help of computers date back to at least the 1990s with many ingenious approaches undertaken since then.

There are two general schools of thought about the analog design problem. In the "classic" approach, a computer program performs *in silico* reactions to produce virtual molecules. The reactions are typically applied in the "forward" direction (starting from some static collections of starting materials[19–25]) and generate molecular spaces which, nowadays, can be quite enormous[25] (*e.g.*, a few billion virtual molecules in Enamine's REAL space and up to 10 (ref. 20) in Merck KGaA's MASSIV collection). These spaces are subsequently pruned for target similarity or other properties of interest. There are also solutions that use retrosynthetic pathways of the parent as input and generate analogs by replacing the original starting materials by structurally or functionally similar blocks.[26] The second family of approaches relies on the burgeoning generative AI models.[27–34] These methods often combine target-similarity with concurrent predictions of other properties.[35] While the very synthesizability of the generated structures has historically been a challenge,[36–39] there has been significant recent progress, as detailed in an excellent recent ref. 40. We observe, however, that irrespective of the approach taken, studies in this area are rarely accompanied by experimental validations of computer-designed syntheses (see ref. 23, 24 and 41) and/or of the predicted potency of the proposed analogs. Such validations are urgently needed as, ultimately, they will decide wider adoption

[a]Institute of Organic Chemistry, Polish Academy of Sciences, Warsaw, Poland. E-mail: anna.zadlo@icho.edu.pl

[b]Allchemy, Inc., Highland, IN, USA

[c]Center for Algorithmic and Robotized Synthesis (CARS), Institute for Basic Science (IBS), Ulsan, 44919, Republic of Korea. E-mail: nanogrzybowski@gmail.com

[d]Department of Chemistry, Ulsan Institute of Science and Technology, UNIST, Ulsan, 44919, Republic of Korea

† Electronic supplementary information (ESI) available. See DOI: https://doi.org/10.1039/d5sc00070j

‡ Authors contributed equally.

of these methods (which, one may argue, is not guaranteed given the widely publicized, recent setbacks of AI in industrial drug discovery[42]).

With this in mind, the overriding objective of our current work is not to argue for the advantages or disadvantages of any particular approach (they all have some) but to test by experiment the particular analog-design pipeline we have been developing for several years now. This pipeline is along the abovementioned "classical" lines of *in silico* synthesis and encompasses substructure replacements within the parent (to diversify the parent scaffold and, hopefully, enhance biological activity), retrosynthetic generation of substrates retaining mutual reactivity, "guided" forward synthesis to produce large numbers of easily synthesizable structural analogs of the parent, and estimation of these candidates' binding affinity to the desired target. Within this scheme, the two key questions we ask relate to the correctness of the computer-designed analog syntheses and to the accuracy of predicting their binding affinities.

Considering two parent molecules (Ketoprofen and Donepezil), the outcomes of our studies are nuanced. On the positive side, experiments validate concise, computer-designed syntheses of seven analogs of Ketoprofen and five analogs of Donepezil (against one failed route). Six Ketoprofen analogs are μM binders to human cyclooxygenase-2 (COX-2), with one

offering slightly better binding than the parent drug (0.61 μM *vs.* 0.69 μM). For Donepezil, all five analogs show sub-micromolar binding to acetylcholinesterase, AChE, with one having nanomolar affinity close to that of the parent (36 nM *vs.* 21 nM). At the same time, binding predictions – which had guided selection of analogs for synthesis validation – by three different docking programs and a neural-network, match the experimental values only to within an order-of-magnitude. These results make us conclude that (i) the synthesis-planning aspects of computerized analog design are nowadays robust, and (ii) common affinity-prediction tools may help select promising binders but cannot discriminate between moderate (μM) *vs.* high-affinity (nM) ones.

2. Results

2.1 Components of the computational pipeline (Fig. 1)

2.1.1 Guided reaction networks. Our analog-design algorithm rests on the application of the so-called guided reaction networks, described in several of our prior works.[43–45] Briefly, assuming a given collection of starting materials ("zero-th synthetic generation," G_0) – whose choice we will discuss in point 1.2 – the algorithm iteratively applies its knowledge-base of reaction transforms, $\{R_i\}$, in the "forward" direction (these reaction transforms are encoded as described in detail in ref. 46
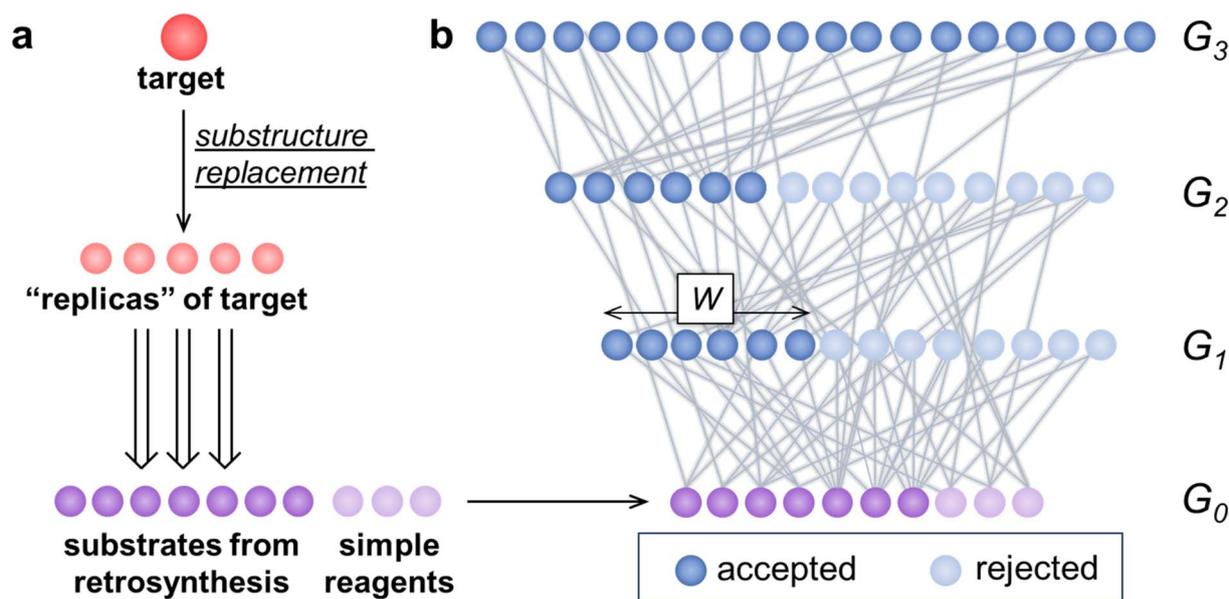

Fig. 1 Scheme of the algorithmic pipeline for substrate selection and subsequent analog generation. (a) For a given target/"parent" of interest (node colored in red), the algorithm first identifies its substructures that can be altered by replacements likely to result in activity enhancement.[49] This creates several (for a typical drug-like parent, ~10–100) parent replicas (light red). The algorithm then expands retrosynthetic networks to find viable synthetic routes to all of these molecules and retains their commercially available starting materials. Since easily makeable analogs are ultimately sought, retrosynthesis is limited to the depth of five steps and using only 180 reaction classes popular in medicinal chemistry. Retrosynthetic searches stop when reaching commercially available substrates, here, those from Mcule's catalog, https://mcule.com/database/, of ~2.5 million chemicals. The set of retrosynthetically-derived substrates (nodes colored violet) is further augmented by 23 simple yet synthetically useful chemicals (here, additional nodes colored in light violet). (b) All of the said substrates serve as the zero-th generation, G_0, for the guided forward search in which, after each round of reactions, only some W molecules most similar to the parent are retained (dark-blue nodes, here $W = 150$). In this way, the forward synthesis is gradually "focused" towards parent's structural analogs. We note that because of this truncation, the sizes of the networks do not explode. This also allows the use of larger collections of reaction transforms (here, ~25 000 rules from Allchemy) to achieve more synthetically diverse outcomes, while limiting the times of network propagation, typically to several minutes.

and 47). Application of $\{R_i\}$ to G_0 gives products in generation G_1. Then, molecules in G_0 and G_1 are combined and become available for yet another round of reactions. If this process is simply repeated without any additional restrictions to create G_2, G_3, *etc.*, the numbers of molecules produced in each generation and the overall size of the network increase very rapidly (as we showed in ref. 43, stronger than exponentially), and the calculation times become impractically long. Instead, to allow for efficient (minutes) exploration of the structural space yet to "guide" network expansion towards the desired "parent", the numbers of products retained after each generation is restricted to some predetermined number W (a.k.a. "beam width"[48]) of those most similar to the said parent molecule. For instance, starting from 100 substrates in G_0, one typically produces thousands of molecules already in G_1 – however, only a few hundred most parent-similar ones are retained as G_1, and allowed to further react with each other and with the G_0 substrates to generate G_2. Regarding this scheme, we note that after a few initial generations, the produced molecules may become already as large as the parent itself. At this point, it makes little sense to allow them to further react with each other. Accordingly, after 1–2 initial generations, we impose an additional constraint that the molecules retained in a given G_i can react only with species of "earlier" generations (*i.e.*, up to G_{i-1}) but no longer between themselves.

2.1.2 Retrosynthesis and the choice of substrates. The second pillar of our approach is the very choice of the G_0 commercially available starting materials, which we wish to select judiciously (to offer the best chance of generating parent's structural analogs) yet automatically (to avoid subjective and tedious selection by software's human operator). This substrate set cannot be too large (as this might explode the forward networks) but should also be (i) diverse, capturing not only the key structural motifs of the parent (*e.g.*, rings or ring systems) but also motifs similar to them; and (ii) should be synthetically flexible, in the sense that the blocks should be able to engage in mutual reactions as much as possible and also in other reactions that functionalize these blocks.

Given these requirements, the straightforward method of disconnecting the parent into the starting materials by retrosynthesis may be overly simplistic. Retrosynthesis of only the parent molecule generates substrates that, in the forward direction, can be reassembled into the parent itself, into some intermediates *en route* to this parent, and usually some molecules in which alternative reactions of the starting materials are performed. However, this approach does not generate diverse analogs. The set of starting materials can, of course, be diversified by adding molecules similar to those found by retrosynthesis – we tested this approach early on but many of the "similars" to the starting materials featured functional group patterns that were unsuitable or problematic for the subsequent forward synthesis (see ESI, Section S2†). Mindful of this, we augmented the retrosynthetic protocol in two ways:

First, by performing substructure replacements (intended to enhance biological activity and digitized, in large part, according to Novartis' tables from ref. 49) within the parent and only then performing retrosyntheses of these "replica" molecules.

The replacements are performed at either peripheral groups or internal motifs such as 1,3-disubstituted benzene rings or piperazines (see ESI, Fig. S2†). They increase structural diversity of the starting materials while, simultaneously, retaining functional groups necessary for the "mix-and-match" reactivity between blocks derived from different replicas. Here, in all retrosyntheses, we used the Allchemy algorithm[50] although other reliable retrosynthetic engines[2–4,51] can be used.

Second, by adding to G_0 some simple yet synthetically useful chemicals with which to further modify and/or activate molecules within the forward networks. While various choices are possible, we used a static, "minimal" set of 23 popular chemicals (see ESI, Fig. S4†) chosen for synthetic versatility. For example, *N*-chlorosuccinimide, *N*-bromosuccinimide and nitric acid enable electrophilic aromatic substitutions, bis(pinacolato)diboron opens the way to Suzuki couplings, DAST can functionalize molecules with fluoride, mesyl chloride activates alcohols for S_N2 reaction, ethyl magnesium bromide can engage in Kulinkovich cyclopropanation while hydrazine, thiourea, azide and trimethyl orthoformate enable formation of various heterocycles, *etc.* An example of a search with and without these additional chemicals in provided in the ESI, Section Section S3.†

2.1.3 Property evaluation. After the retro-forward searches produce the structural analogs, these candidates can be inspected by various substructure filters and ranked by property estimation algorithms, some of which will be discussed in specific examples below.

Regarding the synthesis components 1.1 and 1.2, we note that retrosynthesis may be significantly slower than guided network expansion. With Allchemy's full reaction database, retrosynthetic analysis of a typical drug-like molecule takes only 1–5 min, but for the tens of replicas created in the first stage of the pipeline, these times are already in hours – that is, much longer than for the forward synthesis up to 3–4 generations (4–6 min). Consequently, these two elements of the pipeline use different sets of reaction rules: for retrosynthesis, to reduce the size of retrosynthetic search networks, only 180 reaction classes most popular in medicinal chemistry, and for the forward synthesis, all 25 307 reaction rules available in Allchemy. In this way, both retrosynthetic and forward searches complete within minutes which, based on the feedback on the pipeline's external users appears to be a practically acceptable limit for this type of application. The entire pipeline, integrated in a form of a user-friendly WebApp is available for academic testing at **https://analogs.allchemy.net/** with the user manual provided in the ESI, Section S1.† The source-code for guided network expansion is deposited at **https://zenodo.org/records/7371247**.

2.3 Application of the pipeline to specific targets

We applied the above approach (1)–(3) to identify readily synthesizable analogs to anti-inflammatory Ketoprofen and to Donepezil, a medication used to treat Alzheimer-type dementia.

2.3.1 Ketoprofen analogs. In this example, the algorithm commenced by generating 61 Ketoprofen's substructure-replacement replicas (Fig. 2a). The retrosynthetic searches to all these targets were allowed to terminate at relatively large,
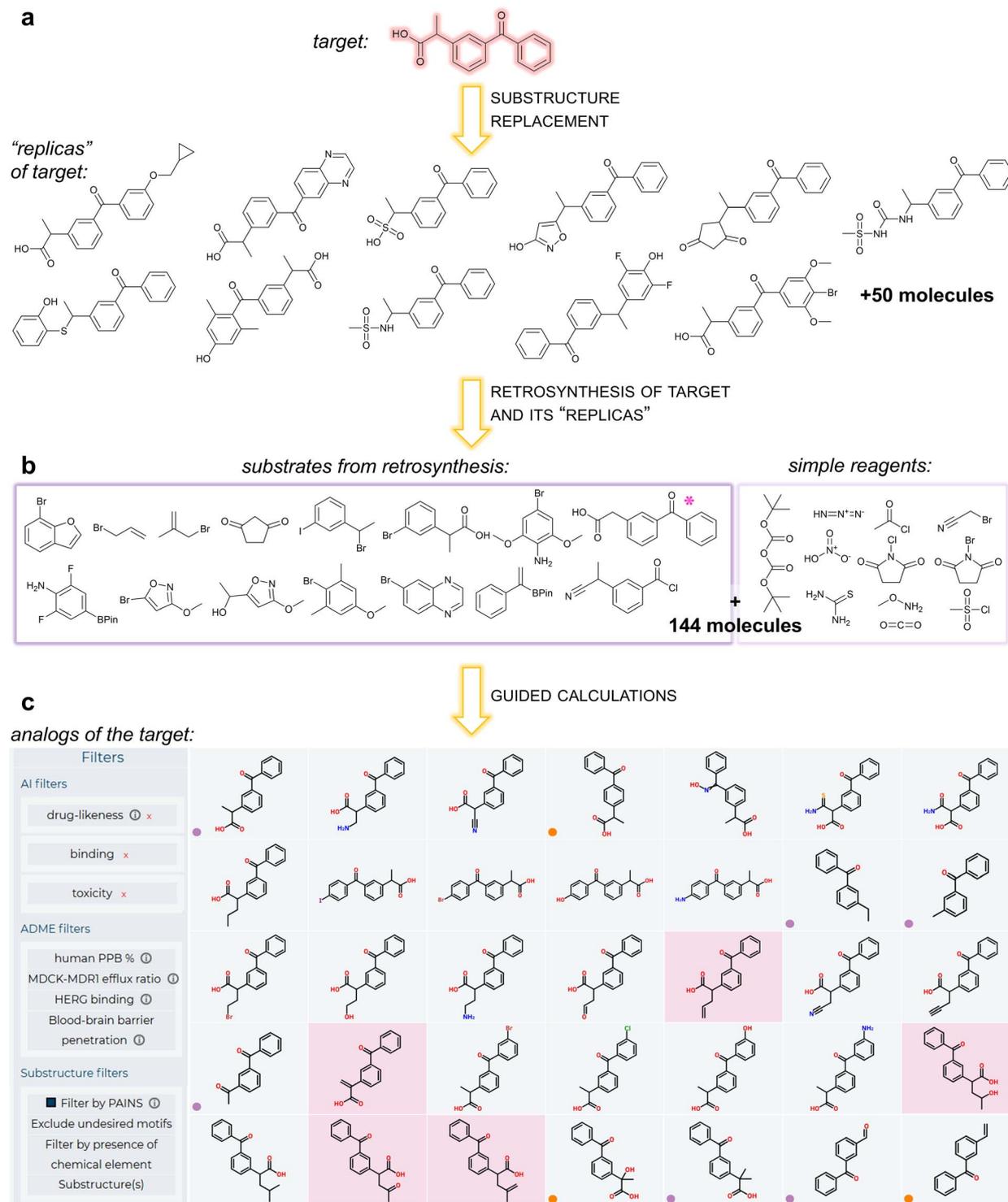
Fig. 2 Search for Ketoprofen's analogs. The panels illustrate the key steps along the analog design pipeline: (a) Ketoprofen and some of its replicas featuring substructure replacements aimed at enhancing biological activity;[49] (b) some of the substrates derived by retrosynthesis of molecules from (a) as well as, on the right, examples of the simple reagents with which to functionalize or activate the substrates (for all 23, see ESI, Fig. S4†); (c) Allchemy screenshot of some of the top-ranking analogs generated by guided expansion of a reaction network starting from molecules in (b). The analogs shown here are sorted by similarity to the Donepezil parent and are centered around the 2-(3-benzoylphenyl)acetic acid with modifications introduced mostly in the α-position of carboxylic acid and as substituents on the aromatic ring. Clicking on any of the "tiles" provides synthesis details (these and other options to visualize the synthetic networks are detailed in the ESI, Section S1†). Some of the analogs ultimately committed to synthesis are shown on pink backgrounds. Visible on the left is the panel with medicinal–chemical functionalities by which the analogs can be filtered (e.g., general drug-likeness,[79] binding to specific proteins, various ADME-Tox models, PAINS and substructure-based filters, see user manual in the ESI†).
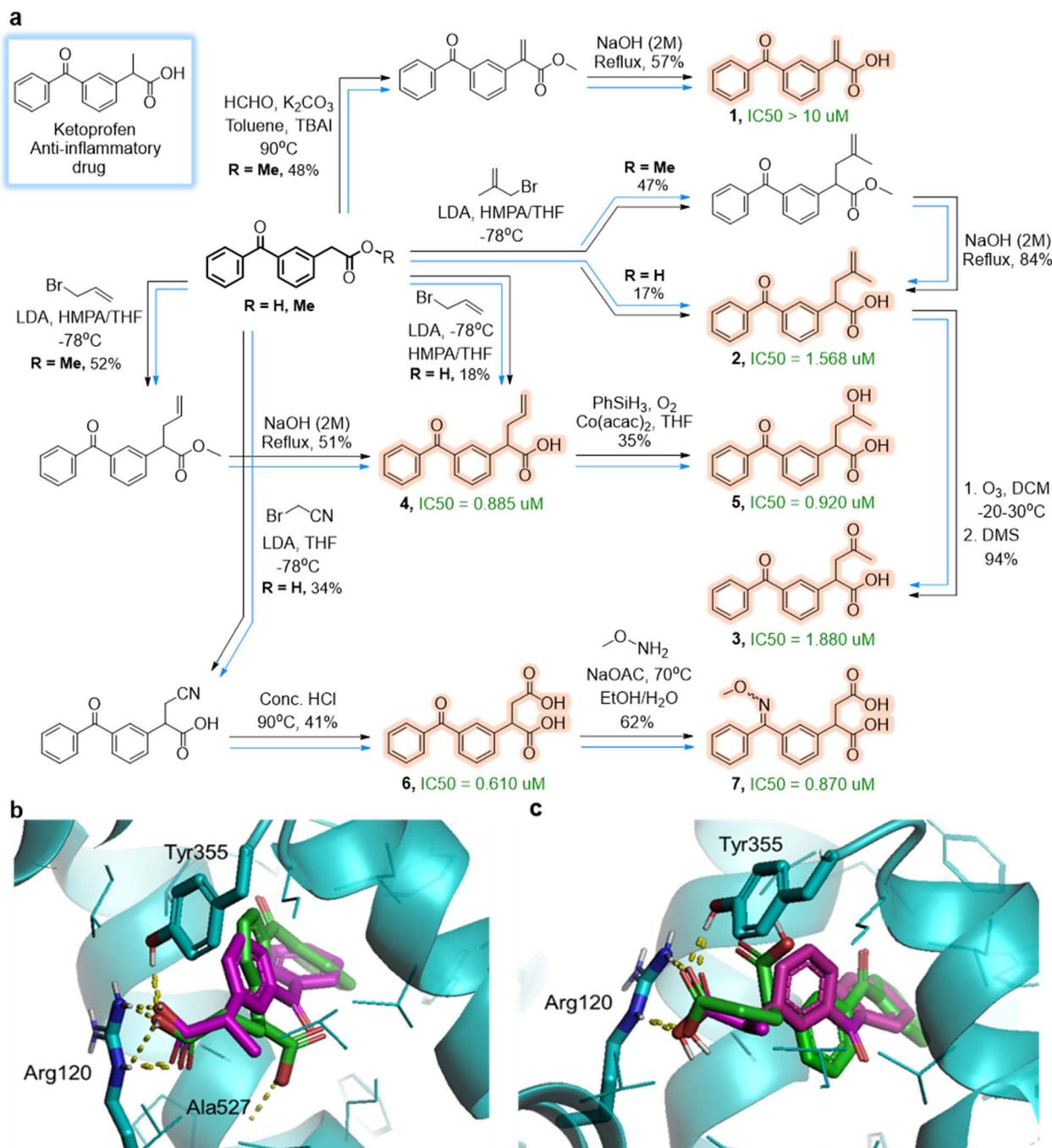
Fig. 3   Ketoprofen's analogs committed to synthesis. (a) A small network of algorithm-planned syntheses of analogs **1** through **7** starting from 2-(3-benzoylphenyl)acetic acid and/or ester derivatives (R = H or R = Me). Experimental pathways (tracked by black arrows) follow the algorithm's original suggestions (blue arrows). Conditions and isolated yields are given next to reaction arrows. IC_{50} values are given next to the analogs. (b) and (c) All analogs were docked into COX-2 protein. The alignment of docking poses from AutoDock 4 for (b) (*S*)-Ketoprofen and its analog (*S*)-**6**, and (c) (*R*)-Ketoprofen and its analog (*R*)-**6**. Key, protein–ligand hydrogen bonds are depicted as yellow dotted lines. The carboxylic acid moiety of (*S*)-Ketoprofen (colored in magenta) forms two hydrogen bonds with Arg120 and one with Tyr355. Its analog (*S*)-**6** (b, colored in green) is predicted to be similarly positioned inside the active site and to form three hydrogen bonds: with Arg120, with Tyr355 and, for the second carboxylic acid moiety, with Ala527. For (*R*)-Ketoprofen (colored in magenta in panel (c)) and its analog (*R*)-**6** (colored in green), the carboxylic acid moieties in both compounds form two hydrogen bonds (with Arg120 and with Tyr355). Raw files with these and all other docking experiments using AutoDock 4, AutoDock Vina, and Dock 6 (ref. 54–57) are deposited at https://zenodo.org/records/14571461.

commercially available starting materials such as (3-benzoylphenyl)acetic acid marked by pink asterisk in Fig. 2b; other notable substrates included allyl bromide derived by retrosynthesis of replicas containing cyclopropylmethoxy substituent.

The 62 retrosynthetic searches took 4 min 20 s (on a server with Intel Xeon Gold 5412U processor) and identified 151 starting materials. Then, the forward search from these substrates and additional set of 23 useful chemicals (four molecules

overlapped between these two sets) was propagated to G_3 and produced, within 4 min 3 s, a guided reaction network encompassing 3692 products of which 781 (21%) had similarity to parent above 0.7 (ECFP6 (ref. 52) – based on Tversky's similarity with parameters (0.2, 0.8); see examples in Fig. 2c and results deposited under the "saved results" tab of the WebApp at https://analogs.allchemy.net/).

Within this set, we focused on molecules 1–7 that form a small synthetic cluster summarized in Fig. 3a. These analogs are all derivatives of the commercially available 2-(3-benzoyl-phenyl)acetic acid and were not reported or tested for cyclooxygenase-2, COX-2, binding before (only compound 1 was synthesized in ref. 53 but in the context of hydrocarboxylation methodology with no biological studies). Moreover, the proposed syntheses all appear concise and straightforward, and were successfully carried out in yields indicated next to the arrows (under conditions identical or very similar to those suggested by the software and without thorough optimization).

In selecting these particular structures, we were also guided by predictions of their binding affinities to COX-2. To this end, we used three popular docking programs, AutoDock 4, Auto-Dock Vina, Dock 6.[54–57] These programs used the 5IKR PDB structure and predicted the binding scores of the analogs 1–7 (averaged over possible stereoisomers of a given racemic analog) to be comparable or more favorable than those of Ketoprofen, which we also docked for reference (top portion of Table 1). Inspection of the docking poses (see examples in Fig. 3b and c and remaining analogs deposited at https://zenodo.org/records/14571461) revealed that these molecules should, indeed, be able to engage in numerous favorable interactions with the COX-2 active site. In parallel, we sought binding strength estimates using Allchemy's neural network, NN, trained on 1 752 921 protein assays from the ChEMBL 29 database[58] and spanning activity values for 3843 one-hot-encoded targets and 863 471 ligands represented as concatenation of Morgan fingerprints with radius 3 (using AllChem.-GetMorganFingerprint function in RDKit[59]), Xfp pharmacophore fingerprints[60] and selection of MACCS keys.[61] The architecture of this feedforward multitasking NN is similar to the one used in ref. 62 and 63, where it was shown to provide the best performance for ChEMBL activity prediction. The main difference is that we used batch normalization, and assigned different activity thresholds to different protein families (according to the values defined in ref. 64). These alterations slightly improved performance to ROC AUC = 0.87. Here, this network predicted that the affinities of the analogs we synthesized should be on-the-order-of micromolar.

To verify these predictions, we ran spectrofluorometric COX-2 human inhibition assay[65,66] and quantified the IC_{50} values. These values are marked in green next to the specific analogs in Fig. 3a. As seen, one analog, 1, is binding poorly, >10 μm, but the remaining six are micromolar binders with one, 6, exhibiting slightly better affinity than the parent Ketoprofen, 0.61 μM vs. 0.69 μM.

Table 1 Predicted binding affinities (or docking scores) and selected medicinal–chemical properties for the parent compounds and their analogs. Top part of the Table is for Ketoprofen and its analogs 1–7; bottom part is for Donepezil and its analogs 11, 14, 16. The first two columns specify, respectively, K_i values predicted by AutoDock Vina and by AutoDock 4. The third column has the docking score from Dock 6. The values shown are averages over all stereoisomers (files with the docked individual stereoisomers are deposited at https://zenodo.org/records/14571461). The remaining four columns give the Allchemy-predicted values of log P calculated by group contribution method[80] as well as predictions of Allchemy's machine-learning models for hERG cardiotoxicity (on a 0–1 scale), degree of human plasma protein binding, hPPB, related to drug absorption and efficacy (0–100%), and degree of blood–brain barrier, BBB, penetration (0–1). Although none of the models used Ketoprofen or Donepezil molecules for training/testing, the key predictions match experimental data. For instance, the hERG model correctly predicts Donepezil to be cardiotoxic (values close to 1), which is in line with experimental studies evidencing that Donepezil binds to hERG[81] with IC_{50} = 1.3 μm and can cause QTc prolongation.[82] By contrast, the model predicts low values of hERG inhibition for Ketoprofen (and its analogs), which agrees with experiments confirming its low cardiotoxicity.[83] In turn, the hPPB model predicts high, >90% bound fractions for both Ketoprofen and Donepezil and their analogs – while lower hPPB values are, in principle, desired in drug design, these predicted values agree with experimental measurements for Ketoprofen (99%[84]) and Donepezil (95.6%[85]). In turn, the blood–brain barrier, BBB, penetration model predicts high values for Donepezil, which is expected for a CNS drug and experimentally confirmed.[86] Ketoprofen also crosses the BBB[87] but we note that some of the analogs, more polar ones, are predicted to have significantly lower values

| Compound	K_i AutoDock Vina (μM)	K_i AutoDock (μM)	Dock 6 (score)	log P	hERG (0–1)	hPPB (0–100%)	BBB (0–1)
Ketoprofen	0.613	0.284	−33.03	3.106	0.04	98.40 ± 1.20	0.91
1	0.413	0.202	−34.85	3.015	0.03	98.50 ± 1.00	0.84
2	0.814	0.268	−34.62	4.052	0.1	98.80 ± 1.30	0.64
3	0.579	0.161	−33.40	3.065	0.01	97.00 ± 1.30	0.42
4	1.138	0.224	−34.82	3.662	0.09	98.60 ± 1.20	0.69
5	0.538	0.348	−36.74	2.857	0.01	94.30 ± 1.20	0.46
6	0.451	0.154	−33.19	2.561	0	96.50 ± 2.70	0.37
7	0.534	0.264	−39.15	2.728	0	95.80 ± 3.60	0.29
Donepezil	0.046	0.037	−43.78	4.361	0.96	91.70 ± 1.30	0.92
11	0.086	0.061	−41.76	4.357	0.98	90.80 ± 1.10	0.9
12	0.064	0.069	−42.54	4.671	0.95	95.80 ± 1.20	0.75
13	0.204	0.097	−43.06	3.722	0.92	88.90 ± 1.10	0.66
14	0.037	0.053	−42.55	3.930	0.92	93.90 ± 4.70	0.77
16	0.027	0.011	−46.98	3.833	0.97	89.60 ± 1.20	0.75
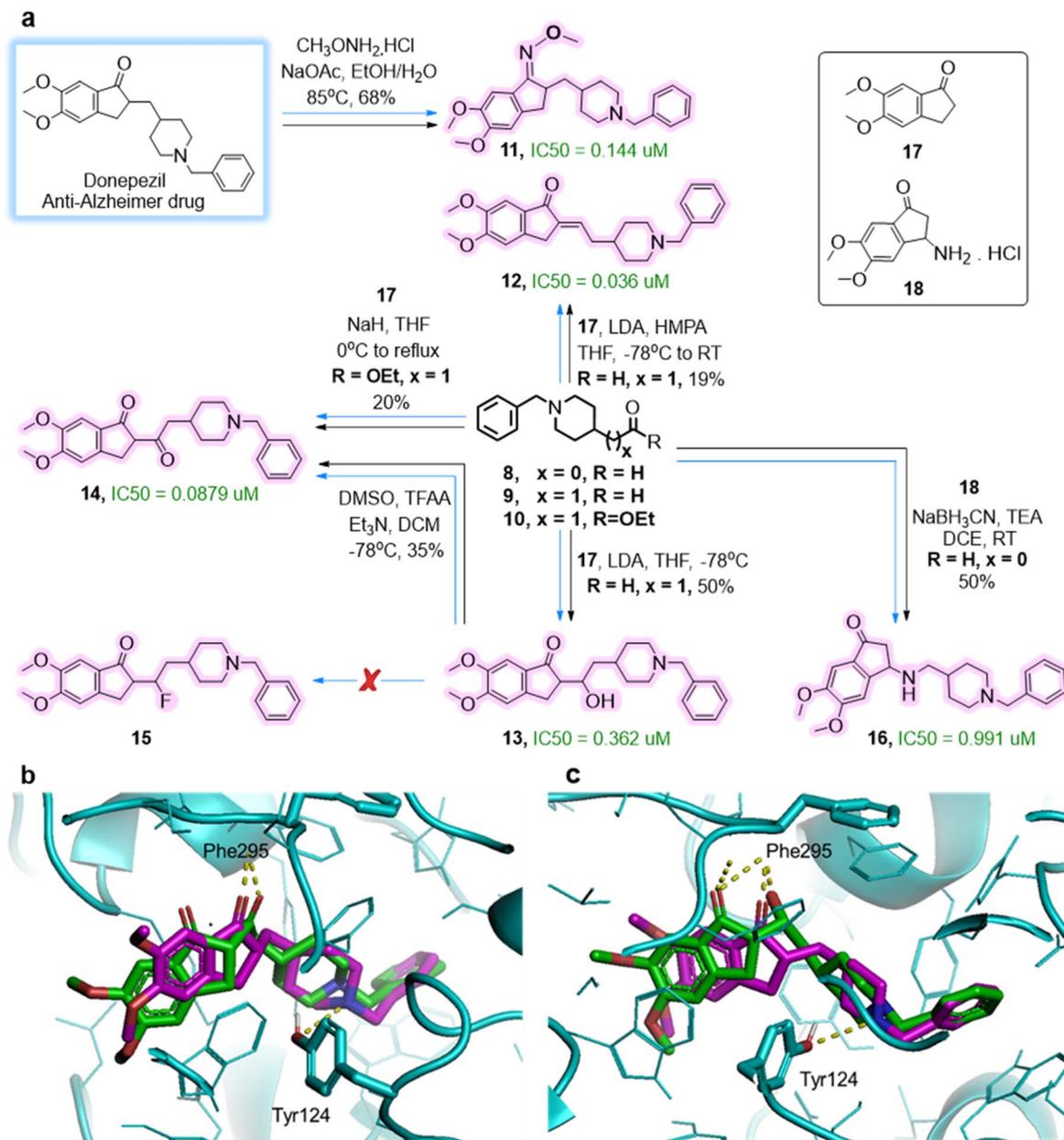
Fig. 4 Donepezil's analogs committed to synthesis. (a) A small network of algorithm-planned syntheses of analogs **11** through **16**. Blue arrows highlight Allchemy's suggestions, black arrows highlight the experimentally executed pathways. Conditions and isolated yields are given above reaction arrows. IC_{50} values are given next to the analogs. Note: As synthesis of **9** and **10** from simpler starting materials was previously described, we followed the literature procedure (**10** was made in two steps and aldehyde **9** from ester **10** in another 2 steps with Allchemy-proposed alcohol as an intermediate; ester **10** and alcohol are commercially available but relatively expensive). All analogs were docked into acetylcholinesterase from *Electrophorus electricus*. Docking poses from AutoDock Vina are aligned for (b) (*R*)-donepezil and its analog (*S*)-**14**, and (c) (*R*)-donepezil and its analog (1*R*,2*S*)-**13**. Key, protein-ligand hydrogen bond interactions are traced by yellow dotted lines. The carbonyl oxygen of (*R*)-Donepezil's (colored in magenta) indanone ring forms a hydrogen bond with Phe295 –NH whereas nitrogen from piperidine ring hydrogen-bonds with Tyr124 –OH. Its analog (*S*)-**14** (b, colored in green) forms hydrogen bonds with Phe295 –NH, but instead of carbonyl oxygen from indanone ring, carbonyl oxygen from 2-(1-benzylpiperidin-4-yl)acetyl side chain is involved. Analog (1*R*,2*S*)-**13** (c, colored in green) forms two hydrogen bonds between Phe295 –NH and carbonyl oxygen of indanone ring and hydroxyl oxygen of analog's side chain as well as and one hydrogen bond between carbonyl oxygen of indanone ring and Arg296 –NH₂. Raw files with these and all other docking experiments using (AutoDock 4, AutoDock Vina, Dock 6)[54–57] are deposited at https://zenodo.org/records/14571461.

2.3.2 Donepezil analogs. We followed a similar protocol as for Ketoprofen. The algorithm generated 18 substructure-replacement replicas of the Donepezil parent. To reach commercially available substrates, the algorithm used

disconnections more central than in Ketoprofen example and reached, *e.g.*, 5,6-dimethoxy-2,3-dihydro-1*H*-inden-1-one, **17**, as well as, 2-(1-benzylpiperidin-4-yl)ethanol and (1-benzylpiperidin-4-yl)acetic acid, that can be easily transformed

into aldehyde **9** – the core substrate, used in most syntheses – and ester **10**, respectively.

Retrosyntheses of the parent and all 18 replicas took only 3 min and generated 44 substrates which were combined with 23 synthetically useful, simple chemicals. Three molecules overlapped between these two sets so that the number of unique starting materials in G_0 was 64. The forward search up to G_3 generated, within 5 min, a network of 3619 products of which 2222 ($\sim$61%) had similarity to parent above 0.7.

Fig. 4a shows six molecules that were committed to synthesis: the replica **11** of the parent drug and analogs **12–15** forming a small cluster entailing only six reactions based on the afore-mentioned aldehyde **9**, ester **10** as well as ketone **17**. Additionally, we included the synthesis of analog **16** that had been found by an earlier version of the algorithm, and used **8** and **18** as starting materials. All these reactions were executed under computer-suggested conditions, save for the Swern rather than Dess–Martin oxidation of **13** to **14**. In five out of six cases, the reactions gave the expected products although in poor to moderate yields (no condition optimization was attempted). In one case, the fluorinated derivative **15** was not obtained because of elimina-tion to **12**. While there are literature examples of fluorination proceeding on β-hydroxy ketones, Allchemy's pK_a model[67] predicts that the cH position within our cyclic aryl ketone is more acidic, hence promoting elimination *vs.* substitution.

As in the case of Ketoprofen, these analogs were chosen because most were not reported before (compound **11** is known as an intermediate in the synthesis of acetylcholinesterase, AChE, inhibitors but its activity was not evaluated[68]) and because their predicted binding scores (by AutoDock 4, Auto-Dock Vina, Dock 6)[54–57] were comparable or better than those of the Donepezil parent, which we also docked for reference (see bottom portion of Table 1). Allchemy's neural network also predicted micromolar-level binding.

These predictions were verified in spectrophotometric AChE inhibition assay,[65,69] which quantified the IC$_{50}$ values given next to the specific analogs in Fig. 4a. The replica **11** had IC$_{50}$ = 144 nM and two analogs were submicromolar, 991 nM for **16** and 362 nM for **13**. However, the two remaining analogs were significantly more potent, 88 nM for **14** and 36 nM for **12**. This last value rivals the potency measured for Donepezil itself, 21 nM.

3. Discussion and conclusions

The above results substantiate three major conclusions. First, the quality of synthetic predictions appears satisfactory with 12 out of 13 analogs made according to the computer-designed routes. This is perhaps not unexpected given that predictions of programs such as Allchemy or Chematica/Synthia had previously been validated on targets more challenging than our analogs.[3,8,10,44] In this light, one can argue that all these simple syntheses could have been designed without much effort by a human expert – while this is true, the computer may be viewed as a useful "calculator" accelerating the straightforward but otherwise tedious steps of the design process, from the creation of replicas *via* substructure replacements, through the selection of commercially available substrates, to forward synthesis.
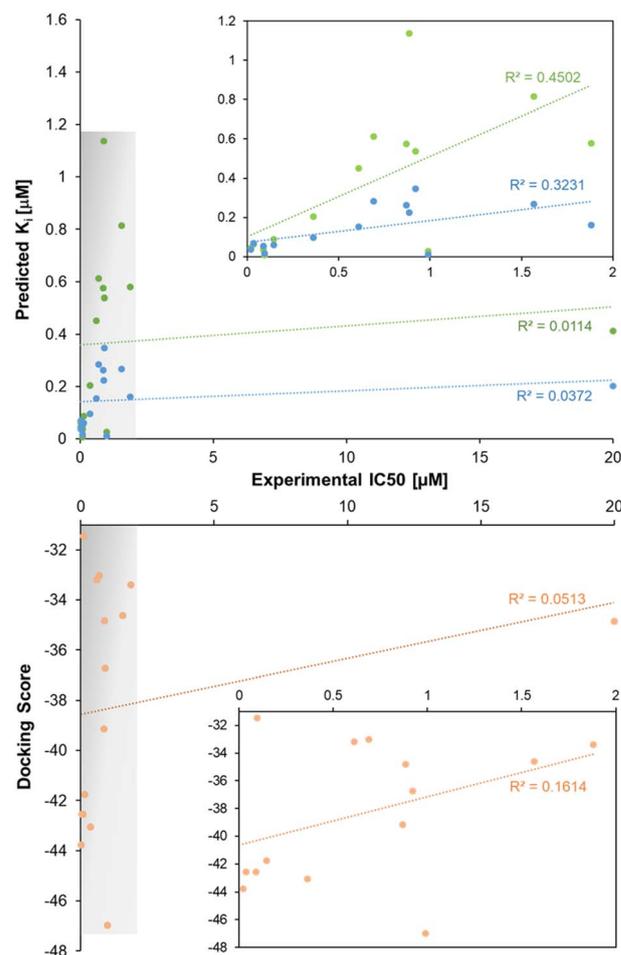

Fig. 5 The relationship between the experimental IC$_{50}$ (μM) and K_i (μM) values (from AutoDock 4, blue, and AutoDock Vina, green) or the docking scores (from Dock 6, orange). Insets zoom on the regions which, in the full plots, are shaded in gray and do not include the poorly binding analog.

Second, whereas the synthesis part is robust, the prediction of analog's properties remains challenging. This is illustrated in Fig. 5 which plots the experimentally measured IC$_{50}$'s against the predictions of the docking programs – as seen, the corre-lations are quite poor and even discounting the outlier **1**, are limited to $\sim$0.45 for AutoDock Vina (green markers in the inset to the upper plot). We observe that such values are in line with comparative studies of docking methods[70] where similar, low correlations were reported. In parallel, Allchemy's internal neural network trained on 1.75 million of protein assays from ChEMBL estimated the potency of our analogs to be micro-molar, which is true for most but not all of them (*e.g.*, not for **1** which is >10 μM and not for **12** and **14** for which IC$_{50}$ values are in tens of nM). Taken together, these results reinforce the view that neither the docking nor NN models can currently predict the affinity accurately – though they can perhaps be accurate to the order-of-magnitude, which can still be useful in dis-tinguishing very poor from decent binders.

Third and last, it should be remembered that in developing potential drugs, binding affinity is but one of the important

metrics and one should also evaluate ADME-Tox properties. There are nowadays multiple machine-learning models to evaluate these properties (*e.g.*, ref. 71–73 for hERG models, ref. 74 for plasma protein binding, PPB, or ref. 75–78 for blood–brain barrier, BBB, penetration) and some have also been implemented in Allchemy's pipeline (see user manual in ESI, Section S1†), offering respectable accuracies ~0.8–0.9 and realistic predictions (see Table 1 and its caption). Thus, one could also think of using these metrics as part of a multi-objective scoring function[35] to guide the synthesis of molecules that, ultimately, meet several desirable criteria at once. The multiobjective approach is, arguably, more conceptually elegant than the synthesize-and-then-evaluate pipeline we pursued here. On the other hand, it should be noted that ADME-Tox models suffer from the scarcity of publically available data (typically, few thousand molecules per model) and are largely untested (and likely less reliable) in out-of-box predictions. Using such metrics to make decisions about which molecules to synthesize can eliminate some interesting candidates from consideration. Our thinking when developing the "synthesis-first" pipeline was that synthesis planning – being the most robust component – should be unhindered by additional constraints, especially that it yields large collections of candidate molecules in very short times. These molecules can then be evaluated by other models/filters, with a human expert making choices which metrics to prioritize (or trust). This said, we recognize that if much larger synthetic spaces are to be explored (with much bigger substrate sets or higher beam width, W, see ref. 44 and 45), then multiobjective scoring should be considered to narrow down and accelerate this exploration.

Data availability

All docking poses are deposited at **https://zenodo.org/records/14571461**. The source-code for guided network expansion is deposited at **https://zenodo.org/records/7371247**. Sample of the database of reaction templates is deposited at **https://zenodo.org/records/15001486**. All synthesis results are deposited under the "saved results" tab of the WebApp at **https://analogs.allchemy.net/**(see user manual in the ESI†). To test the WebApp under two-week, free academic access, please send an email from an academic address to admin@allchemy.net for access credentials.

Author contributions

A. M. and S. M. performed syntheses. A. M. and A. Ż.-D. Performed the binding assays. W. B., A. W., R. R., S. S., M. M, A. K. and K. M. developed the algorithms and the WebApp. A. Ż.-D. performed docking studies and supervised the syntheses. B. A. G. conceived and supervised the project.

Conflicts of interest

W. B., A. W., R. R., S. S., M. M., A. K., K. M. and B. A. G. are consultants and/or stakeholders of Allchemy, Inc. Allchemy software is property of Allchemy Inc.

Acknowledgements

References

1 S. Szymkuć, E. P. Gajewska, T. Klucznik, K. Molga, P. Dittwald, M. Startek, M. Bajczyk and B. A. Grzybowski, *Angew. Chem., Int. Ed.*, 2016, **55**, 5904–5937.

2 C. W. Coley, L. Rogers, W. H. Green and K. F. Jensen, *ACS Cent. Sci.*, 2017, **3**, 1237–1245.

3 T. Klucznik, B. Mikulak-Klucznik, M. P. McCormack, H. Lima, S. Szymkuć, M. Bhowmick, K. Molga, Y. Zhou, L. Rickershauser, E. P. Gajewska, A. Toutchkine, P. Dittwald, M. P. Startek, G. J. Kirkovits, R. Roszak, A. Adamski, B. Sieredzińska, M. Mrksich, S. L. J. Trice and B. A. Grzybowski, *Chem*, 2018, **4**, 522–532.

4 M. H. S. Segler, M. Preuss and M. P. Waller, *Nature*, 2018, **555**, 604–610.

5 C. W. Coley, D. A. Thomas, J. Lummiss, J. N. Jaworski, C. P. Breen, V. Schultz, T. Hart, J. S. Fishman, L. Rogers, H. Gao, R. W. Hicklin, P. P. Plehiers, J. Byington, J. S Piotti, W. H Green, A. J. Hart, T. F. Jamison and K. F. Jensen, *Science*, 2019, **365**, eaax1566.

6 A. F. de Almeida, R. Moreira and T. Rodrigues, *Nat. Rev. Chem.*, 2019, **3**, 589–604.

7 P. Schwaller, A. C. Vaucher, R. Laplaza, C. Bunne, A. Krause, C. Corminboeuf and T. Laino, *Wiley Interdiscip. Rev.: Comput. Mol. Sci.*, 2022, **12**, e1604.

8 B. Mikulak-Klucznik, P. Gołębiowska, A. A. Bayly, O. Popik, T. Klucznik, S. Szymkuć, E. P. Gajewska, P. Dittwald, O. Staszewska-Krajewska, W. Beker, T. Badowski, K. A. Scheidt, K. Molga, J. Mlynarski, M. Mrksich and B. A. Grzybowski, *Nature*, 2020, **588**, 83–88.

9 Y. Lin, R. Zhang, D. Wang and T. Cernak, *Science*, 2023, **379**, 453–457.

10 T. Klucznik, L. D. Syntrivanis, S. Baś, B. Mikulak-Klucznik, M. Moskal, S. Szymkuć, J. Mlynarski, L. Gadina, W. Beker, M. D. Burke, K. Tiefenbacher and B. A. Grzybowski, *Nature*, 2024, **625**, 508–515.

11 P. Jia, J. Pei, G. Wang, X. Pan, Y. Zhu, Y. Wu and L. Ouyang, *Green Synth. Catal.*, 2022, **3**, 11–24.

12 A. Zhavoronkov, Y. A. Ivanenkov, A. Aliper, M. S. Veselov, V. A. Aladinskiy, A. V. Aladinskaya, V. A. Terentiev, D. A. Polykovskiy, M. D. Kuznetsov, A. Asadulaev,

Y. Volkov, A. Zholus, R. R. Shayakhmetov, A. Zhebrak, L. I. Minaeva, B. A. Zagribelnyy, L. H. Lee, R. Soll, D. Madge, L. Xing, T. Guo and A. Aspuru-Guzik, *Nat. Biotechnol.*, 2019, **37**, 1038–1040.

13 D. E. Graff, E. I. Shakhnovich and C. W. Coley, *Chem. Sci.*, 2021, **12**, 7866–7881.

14 T. J. Struble, J. C. Alvarez, S. P. Brown, M. Chytil, J. Cisar, R. L. DesJarlais, O. Engkvist, S. A. Frank, D. R. Greve, D. J. Griffin, X. Hou, J. W. Johannes, C. Kreatsoulas, B. Lahue, M. Mathea, G. Mogk, C. A. Nicolaou, A. D. Palmer, D. J. Price, R. I. Robinson, S. Salentin, L. Xing, T. Jaakkola, W. H. Green, R. Barzilay, C. W. Coley and K. F. Jensen, *J. Med. Chem.*, 2020, **63**, 8667–8682.

15 A. V. Sadybekov and V. Katritch, *Nature*, 2023, **616**, 673–685.

16 R. Roszak, L. Gadina, A. Wołos, A. Makkawi, B. Mikulak-Klucznik, Y. Bilgi, K. Molga, P. Gołębiowska, O. Popik, T. Klucznik, S. Szymkuć, M. Moskal, S. Baś, R. Frydrych, J. Mlynarski, O. Vakuliuk, D. T. Gryko and B. A. Grzybowski, *Nat. Commun.*, 2024, **15**, 10285.

17 T. N. K. Raju, *Lancet*, 2000, **356**, 436.

18 J. Fischer and C. R. Ganellin, *Analogue-Based Drug Discovery II*, Wiley-VCH, 2010, DOI: **10.1002/9783527630035**.

19 M. Hartenfeller and G. Schneider, *Wiley Interdiscip. Rev.: Comput. Mol. Sci.*, 2011, **1**, 742–759.

20 G. Schneider and U. Fechner, *Nat. Rev. Drug Discovery*, 2005, **4**, 649–663.

21 G. Schneider, M. L. Lee, M. Stahl and P. Schneider, *J. Comput. Aided Mol. Des.*, 2000, **14**, 487–494.

22 X. Q. Lewell, D. B. Judd, S. P. Watson and M. M. Hann, *J. Chem. Inf. Comput. Sci.*, 1998, **38**, 511–522.

23 H. M. Vinkers, M. R. de Jonge, F. F. D. Daeyaert, J. Heeres, L. M. H. Koymans, J. H. van Lenthe, P. J. Lewi, H. Timmerman, K. Van Aken and P. A. J. Janssen, *J. Med. Chem.*, 2003, **46**, 2765–2773.

24 M. Hartenfeller, H. Zettl, M. Walter, M. Rupp, F. Reisen, E. Proschak, S. Weggen, H. Stark and G. Schneider, *PLoS Comput. Biol.*, 2012, **8**, e1002380.

25 T. Hoffmann and M. Gastreich, *Drug Discovery Today*, 2019, **24**, 1148–1156.

26 U. Dolfus, H. Briem and M. Rarey, *J. Chem. Inf. Model.*, 2022, **62**, 3565–3576.

27 B. Sanchez-Lengeling and A. Aspuru-Guzik, *Science*, 2018, **361**, 360–365.

28 M. H. S. Segler, T. Kogej, C. Tyrchan and M. P. Waller, *ACS Cent. Sci.*, 2018, **4**, 120–131.

29 I. Goodfellow, J. Pouget-Abadie, M. Mirza, B. Xu, D. Warde-Farley, S. Ozair, A. Courville and B. Yoshua, in *Advances in Neural Information Processing Systems 27 (NIPS 2014)*, 2014, pp. 2672–2680.

30 D. C. Elton, Z. Boukouvalas, M. D. Fuge and P. W. Chung, *Mol. Syst. Des. Eng.*, 2019, **4**, 828–849.

31 J. Bradshaw, B. Paige, M. J. Kusner, M. H. S. Segler and J. M. Hernández-Lobato, *arXiv*, 2019, preprint, arXiv:1906.05221, DOI: **10.48550/arXiv.1906.05221**.

32 T. Blaschke, J. Arús-Pous, H. Chen, C. Margreitter, C. Tyrchan, O. Engkvist, K. Papadopoulos and A. Patronov, *J. Chem. Inf. Model.*, 2020, **60**, 5918–5922.

33 J. Bradshaw, B. Paige, M. J. Kusner, M. H. S. Segler and J. M. Hernández-Lobato, *arXiv*, 2020, preprint, arXiv:2012.11522, DOI: **10.48550/arXiv.2012.11522**.

34 S. K. Gottipati, B. Sattarov, S. Niu, Y. Pathak, H. Wei, S. Liu, K. M. J. Thomas, S. Blackburn, C. W. Coley, J. Tang, S. Chandar and Y. Bengio, *arXiv*, 2020, preprint, arXiv:2004.12485, DOI: **10.48550/arXiv.2004.12485**.

35 J. C. Fromer, D. E. Graff and C. W. Coley, *Digital Discovery*, 2024, **3**, 467–481.

36 W. Gao and C. W. Coley, *J. Chem. Inf. Model.*, 2020, **60**, 5714–5723.

37 P. Renz, D. Van Rompaey, J. K. Wegner, S. Hochreiter and G. Klambauer, *Drug Discovery Today: Technol.*, 2019, **32**, 55–63.

38 W. P. Walters, R. Barzilay and E. Opin, *Drug. Discovery*, 2021, **16**, 937–947.

39 M. Stanley and M. Segler, *Curr. Opin. Struct. Biol.*, 2023, **82**, 102658.

40 W. Gao, S. Luo and C. W. Coley, *arXiv*, 2024, preprint, arXiv:2410.03494, DOI: **10.48550/arXiv.2410.03494**.

41 S. K. Singh, K. King, C. Gannett, C. Chuong, S. Y. Joshi, C. Plate, P. Farzeen, E. M. Webb, L. Kumar-Kunche, J. Weger-Lucarelli, A. N. Lowell, A. M. Brown and S. A. Deshmukh, *J. Phys. Chem. Lett.*, 2023, **14**, 9490–9499.

42 D. Lowe, *AI Does Not Make It Easy (In the pipeline)*, Science, 2024, **https://www.science.org/content/blog-post/ai-does-not-make-it-easy**.

43 A. Wołos, R. Roszak, A. Żądło-Dobrowolska, W. Beker, B. Mikulak-Klucznik, G. Spólnik, M. Dygas, S. Szymkuć and B. A. Grzybowski, *Science*, 2020, **369**, eaaw1955.

44 A. Wołos, D. Koszelewski, R. Roszak, S. Szymkuć, M. Moskal, R. Ostaszewski, B. T. Herrera, J. M. Maier, G. Brezicki, J. Samuel, J. A. M. Lummiss, D. T. McQuade, L. Rogers and B. A. Grzybowski, *Nature*, 2022, **604**, 668–676.

45 R. Roszak, A. Wołos, M. Benke, Ł. Gleń, J. Konka, P. Jensen, P. Burgchardt, A. Żądło-Dobrowolska, P. Janiuk, S. Szymkuć and B. A. Grzybowski, *Chem*, 2024, **10**, 952–970.

46 K. Molga, E. P. Gajewska, S. Szymkuć and B. A. Grzybowski, *React. Chem. Eng.*, 2019, **4**, 1506–1521.

47 F. Strieth-Kalthoff, S. Szymkuć, K. Molga, A. Aspuru-Guzik, F. Glorius and B. A. Grzybowski, *J. Am. Chem. Soc.*, 2024, **146**, 11005–11017.

48 B. A. Grzybowski, T. Badowski, K. Molga and S. Szymkuć, *Wiley Interdiscip. Rev.: Comput. Mol. Sci.*, 2023, **13**, e1630.

49 P. Ertl, E. Altmann, S. Racine and R. Lewis, *Eur. J. Med. Chem.*, 2022, **238**, 114483.

50 B. Mikulak-Klucznik, T. Klucznik, W. Beker, M. Moskal and B. A. Grzybowski, *Chem*, 2024, **10**, 1319–1326.

51 S. Genheden, A. Thakkar, V. Chadimová, J.-L. Reymond, O. Engkvist and E. Bjerrum, *J. Cheminform.*, 2020, **12**, 70.

52 D. Rogers and M. Hahn, *J. Chem. Inf. Model.*, 2010, **50**, 742–754.

53 D. Liu, T. Ru, Z. Deng, L. Zhang, Y. Ning and F. E. Chen, *ACS Catal.*, 2023, **13**, 12868–12876.

54 G. M. Morris, R. Huey, W. Lindstrom, M. F. Sanner, R. K. Belew, D. S. Goodsell and A. J. Olson, *J. Comput. Chem.*, 2009, **16**, 2785–2791.

55 O. Trott and A. J. Olson, *J. Comput. Chem.*, 2010, **31**, 455–461.

56 J. Eberhardt, D. Santos-Martins, A. F. Tillack and S. Forli, *J. Chem. Inf. Model.*, 2021, **61**, 3891–3898.

57 W. J. Allen, T. E. Balius, S. Mukherjee, S. R. Brozell, D. T. Moustakas, P. T. Lang, D. A. Case, I. D. Kuntz and R. C. Rizzo, *J. Comput. Chem.*, 2015, **36**, 1132–1156.

58 *ChEMBLdb*, **http://ftp.ebi.ac.uk/pub/databases/chembl/ChEMBLdb/releases/chembl_29/**, accessed February 28, 2025.

59 G. Landrum, *RDKit*, **http://www.rdkit.org**, accessed February 28, 2025.

60 M. Awale and J.-L. Reymond, *J. Chem. Inf. Model.*, 2014, **54**, 1892–1907.

61 J. L. Durant, B. A. Leland, D. R. Henry and J. G. Nourse, *J. Chem. Inf. Comput. Sci.*, 2002, **42**, 1273–1280.

62 A. Mayr, G. Klambauer, T. Unterthiner, M. Steijaert, J. K. Wegner, H. Ceulemans, D.-A. Clevert and S. Hochreiter, *Chem. Sci.*, 2018, **9**, 5441–5451.

63 N. Bosc, F. Atkinson, E. Félix, A. Gaulton, A. Hersey and A. R. Leach, *J. Cheminform.*, 2019, **11**, 64.

64 K. Yang, K. Swanson, W. Jin, C. Coley, P. Eiden, H. Gao, A. Guzman-Perez, T. Hopper, B. Kelley, M. Mathea, A. Palmer, V. Settels, T. Jaakkola, K. Jensen and R. Barzilay, *J. Chem. Inf. Model.*, 2019, **59**, 3370–3388.

65 S. Asghar, N. Mushtaq, A. Ahmed, L. Anwar, R. Munawar and S. Akhtar, *Molecules*, 2024, **29**, 490.

66 SigmaAldrich, Cyclooxygenase 2 human ≥70% (SDS-PAGE), 0858UN-UN1000UN, **https://www.sigmaaldrich.com/PL/en/product/sigma/c0858**, accessed 8 April 2025.

67 R. Roszak, W. Beker, K. Molga and B. A. Grzybowski, *J. Am. Chem. Soc.*, 2019, **141**, 17142–17149.

68 H. Sugimoto, Y. Iimura, Y. Yamanishi and K. Yamatsu, *J. Med. Chem.*, 1995, **38**, 4821–4829.

69 SigmaAldrich, *Acetylcholinesterase Inhibitor Screening Kit, 324KT-KT1KT*, **https://www.sigmaaldrich.com/PL/en/product/sigma/mak324**, accessed 8 April 2025.

70 A. Pecina, J. Fanfrlík, M. Lepšík and J. Řezáč, *Nat. Commun.*, 2024, **15**, 1127.

71 K. Ogura, T. Sato, H. Yuki and T. Honma, *Sci. Rep.*, 2019, **9**, 12220.

72 H. Kim and H. Nam, *Comput. Biol. Chem.*, 2020, **87**, 107286.

73 X. Zhang, J. Mao, M. Wei, Y. Qi and J. Z. H. Zhang, *J. Chem. Inf. Model.*, 2022, **62**, 1830–1839.

74 Z. Han, Z. Xia, J. Xia, I. V. Tetko and S. Wu, *Eur. J. Pharm. Sci.*, 2025, **204**, 106946.

75 F. Meng, Y. Xi, J. Huang and P. W. Ayers, *Sci. Data*, 2021, **8**, 289.

76 V. Kumar, A. Banerjee and K. Roy, *J. Chem. Inf. Model.*, 2024, **64**, 4298–4309.

77 S. Cherian Parakkal, R. Datta and D. Das, *Mol. Inf.*, 2022, **41**, 2100315.

78 B. Mazumdar, P. K. Deva Sarma, H. J. Mahanta and G. N. Sastry, *Comput. Biol. Med.*, 2023, **160**, 106984.

79 W. Beker, A. Wołos, S. Szymkuć and B. A. Grzybowski, *Nat. Mach. Intell.*, 2020, **2**, 457–465.

80 S. A. Wildman and G. M. Crippen, *J. Chem. Inf. Comput. Sci.*, 1999, **39**, 868–873.

81 Y. J. Chae, H. J. Lee, J. H. Jeon, I.-B. Kim, J.-S. Choi, K.-W. Sung and S. J. Hahn, *Brain Res.*, 2015, **1597**, 77–85.

82 S. M. Vogel, L. M. Mican and T. L. Smith, *Ment. Health Clin.*, 2019, **9**, 128–132.

83 L. Brandolini, A. Antonosante, C. Giorgio, M. Begnasco, M. d'Angelo, V. Castelli, E. Benedetti, A. Cimini and M. Allegretti, *Sci. Rep.*, 2020, **10**, 18337.

84 P. J. Hayball, R. L. Nation, F. Bochner, J. L. Newton, R. A. Massy-Westropp and D. P. G. Hamon, *Chirality*, 1991, **3**, 460–466.

85 S. L. Rogers, N. M. Cooper, R. Sukovaty, J. E. Pederson, J. N. Lee and L. T. Friedhoff, *Br. J. Clin. Pharmacol.*, 1998, **46**, 7–12.

86 W. A. Banks, *Adv. Drug. Del. Rev.*, 2012, **64**, 629–639.

87 H. Kokki, *Pediatric Drugs*, 2010, **12**, 313–329.